

A FRAME BASED BEAM AND PULSED BEAM SUMMATION FORMULATION FOR ULTRA WIDEBAND / SHORT PULSE RADIATION

Amir Shlivinski⁽¹⁾, Ehud Heyman⁽¹⁾, Amir Boag⁽¹⁾, Christine Letrou⁽²⁾

⁽¹⁾ *Department of Physical Electronics, Tel Aviv University Tel Aviv 69978, Israel,
E-mail: samir@eng.tau.ac.il, heyman@eng.tau.ac.il, boag@eng.tau.ac.il*

⁽²⁾ *I.N.T., 9 rue Charles Fourier, F-91011 EVRY Cedex, France, E-mail: Christine.Letrou@int-evry.fr*

ABSTRACT

Two discretized beam summation schemes for ultra-wideband / short-pulse radiation from apertures are presented. One is formulated in the frequency domain and utilizes Gaussian beams propagators and frequency-independent beam lattices, and the other, directly in the time domain utilizing isodiffracting pulsed beams (I-PB). Efficient representation is obtained using a hierarchy of one-octave frequency bands such that the beam lattices are obtained by decimation of the lattice at the highest band. For short-pulse sources the scheme consists of a multiscale hierarchy of decimated sets of space-time I-PB window functions within a discretized slant-stack transform.

1. INTRODUCTION

Beam-based phase space formulations are an important tool for tracking wave fields since they provide a framework for constructing spectrally uniform solutions in complex configurations. In a typical formulation, the field is expanded into a phase-space spectrum of beams that emanate at a given set of points and directions in the source domain, and thereafter are tracked locally in the medium. The underlying theory is that of windowed configuration-spectrum transforms, e.g., the windowed Fourier transform (WFT) in the frequency domain (FD) and the local slant-stack transform (L-SST) in the time domain (TD) [1]. The corresponding *complete set* of propagators are Gaussian beams (GB) or isodiffracting pulsed beams (I-PB), respectively [2]. Localization of the transforms then renders the representations localized about the geometrical optics skeleton.

An important property of the local spectrum formulations is that they are overcomplete and thus may be a priori discretized. In the FD, such discretized formulations have been obtained via the Gabor representation, yet this representation suffers from two *inherent difficulties*: (a) non-locality and instability of the expansion coefficients, and (b) frequency dependence of the beam lattice (as follows from the Gabor condition $\bar{k}_x \bar{x} = 2\pi$ where \bar{x} and \bar{k}_x are the spatial and spectral discretization step-sizes). Property (b) makes the conventional Gabor-based beam formulation *inapplicable* for ultra-wideband (UWB) or TD applications since it requires the tracking of different beams (with different axes) for each frequency [3].

In this paper we present a unified discretized frame formulation for UWB or for TD representations. Such representation *should* satisfy the following requirements [3]: (a) the phase space beam lattice is frequency independent hence the beams need to be tracked only once for all frequencies; (b) the propagators can be tracked locally in the medium and are known in a closed-form either, in the UWB domain or directly in the TD; (c) the expansion coefficients are localized and stable over the entire UWB domain, or they may be calculated directly in the TD via local processing of the source functions.

2. THE BASIC FRAME FORMULATION IN THE ULTRA WIDEBAND (UWB) DOMAIN

The theory is presented here in the context of radiation from a large focused aperture in the $z = 0$ plane with prescribed field $u_0(\mathbf{x}, t)$. The 3D coordinates are denoted as $\mathbf{r} = (\mathbf{x}, z)$ with $\mathbf{x} = (x_1, x_2)$ being the coordinates transverse to z . The frequency spectrum of u_0 is constraint to the band $\Omega = (\omega_{\min}, \omega_{\max})$ that may extend over several octaves.

We consider first the multi-frequency theory where a $e^{-i\omega t}$ time-dependence is assumed. Since the theory is formulated over a wide frequency band, we use the frequency-normalized spatial spectrum coordinate $\boldsymbol{\xi} = \mathbf{k}_x/k$ where $\mathbf{k}_x = (k_{x_1}, k_{x_2})$ is the spectral wave number with $k = \omega/c$, and use the spatial - spectral transforms

$$\widehat{u}_0(\boldsymbol{\xi}; \omega) = \int d^2x \widehat{u}_0(\mathbf{x}; \omega) e^{-ik\boldsymbol{\xi}\cdot\mathbf{x}}, \quad \widehat{u}_0(\mathbf{x}; \omega) = \left(\frac{k}{2\pi}\right)^2 \int d^2\xi \widehat{u}_0(\boldsymbol{\xi}; \omega) e^{ik\boldsymbol{\xi}\cdot\mathbf{x}}, \quad \boldsymbol{\xi} = (\xi_1, \xi_2), \quad (1)$$

where $\widehat{}$ and $\widetilde{}$ denote frequency domain and spatial spectrum constituents, respectively. This defines the *frequency-independent* phase space $\mathbf{X} = (\mathbf{x}, \boldsymbol{\xi})$, where $\boldsymbol{\xi}$ is the spectral direction.

We start by choosing a reference frequency $\bar{\omega}$ such that $\bar{\omega} > \omega_{\max}$ and define a phase-space lattice whose unit cell $(\bar{x}, \bar{\xi})$ satisfies the Gabor condition at $\bar{\omega}$, i.e. $\bar{k}\bar{\xi}\bar{x} = 2\pi$. This choice implies that for all $\omega < \bar{\omega}$ the lattice is overcomplete with

$$\bar{k}_x \bar{x} = k \bar{\xi} \bar{x} = 2\pi\nu < 2\pi, \quad \text{where } \nu = \omega/\bar{\omega} = \text{overcompleteness parameter}, \quad \nu < 1. \quad (2)$$

The phase-space lattice $\mathbf{X}_\mu = (\mathbf{x}_m, \boldsymbol{\xi}_n) = (m_1\bar{x}, m_2\bar{x}, n_1\bar{\xi}, n_2\bar{\xi})$ is *frequency independent*, thereby defining the same beam trajectories for all $\omega < \bar{\omega}$. We use conveniently the vector indices $\mathbf{m} = (m_1, m_2)$, $\mathbf{n} = (n_1, n_2)$, and $\boldsymbol{\mu} = (\mathbf{m}, \mathbf{n})$.

Next, for a proper window function $\hat{\psi}(\mathbf{x}; \omega)$ we introduce the Gabor-type frames

$$\hat{\psi}_\mu(\mathbf{x}; \omega) = \hat{\psi}(\mathbf{x} - \mathbf{x}_m; \omega) e^{ik\boldsymbol{\xi}_n \cdot (\mathbf{x} - \mathbf{x}_m)}, \quad \hat{\varphi}_\mu(\mathbf{x}; \omega) = \hat{\varphi}(\mathbf{x} - \mathbf{x}_m; \omega) e^{ik\boldsymbol{\xi}_n \cdot (\mathbf{x} - \mathbf{x}_m)} \quad (3)$$

The set $\{\hat{\psi}_\mu\}$ constitutes a frame in $L_2(\mathbb{R}) \times L_2(\mathbb{R})$ if $\nu < 1$ [4]. The ‘‘dual function’’ $\hat{\varphi}(\mathbf{x}; \omega)$ corresponding to $\hat{\psi}(\mathbf{x}; \omega)$ is calculated for each ν via the ‘‘frame operator’’ [4] such that $\{\hat{\varphi}_\mu\}$ constitutes also a frame. Unlike the irregular and non-local biorthogonal function in the Gabor limit $\nu \uparrow 1$, for $\nu < 1$ the dual function $\hat{\varphi}_\mu$ is smooth and localized, yielding stable coefficients in (5). It has further been shown in [3] that for a given ν the snuggest frame (tightest frame bounds) is obtained if the window is *matched to the phase space lattice* such that

$$\rho \equiv \frac{\Delta_x/\bar{x}}{\Delta_\xi/\bar{\xi}} = 1, \quad \text{where } \rho \equiv \text{the grid aspect-ratio, and } \Delta_x \text{ and } \Delta_\xi = \text{the spatial / spectral widths of } \hat{\psi}. \quad (4)$$

Other conditions for choosing the ‘‘optimal’’ window for all $\omega < \bar{\omega}$ are discussed in connection with (13) below.

The frame representation of the initial field $\hat{u}_0(\mathbf{x}; \omega)$ and of the propagated field $\hat{u}(\mathbf{r}, \omega)$ for $z > 0$ and $\forall \omega < \bar{\omega}$ is

$$\hat{u}_0(\mathbf{x}; \omega) = \sum_{\boldsymbol{\mu}} \hat{a}_\mu(\omega) \hat{\psi}_\mu(\mathbf{x}; \omega), \quad \hat{u}(\mathbf{r}, \omega) = \sum_{\boldsymbol{\mu}} \hat{a}_\mu(\omega) \hat{B}_\mu(\mathbf{r}; \omega), \quad \text{where } \hat{a}_\mu(\omega) = \langle \hat{u}_0(\mathbf{x}; \omega), \hat{\varphi}_\mu(\mathbf{x}; \omega) \rangle. \quad (5)$$

where $\langle \cdot, \cdot \rangle$ is the conventional inner product in $L_2(\mathbb{R}) \times L_2(\mathbb{R})$. Thus \hat{a}_μ are readily recognized as the local WFT spectrum of \hat{u}_0 about the phase space point \mathbf{X}_μ , with respect to the window $\hat{\varphi}_\mu$. $\hat{\varphi}$ and $\hat{\psi}$ are therefore termed as the ‘‘analysis’’ and ‘‘synthesis’’ windows. The beam propagators $\hat{B}_\mu(\mathbf{r}, \omega)$ are obtained by propagating $\hat{\psi}_\mu(\mathbf{x}, \omega)$: they emerge from the points \mathbf{x}_m in the $z=0$ plane in the directions $\boldsymbol{\xi}_n = \sin \theta_n (\cos \phi_n, \sin \phi_n)$ (cf. Fig. 1). The expansion for $\hat{u}(\mathbf{r}, \omega)$ involves only the propagating beams with $|\boldsymbol{\xi}_n| < 1$ whereas all other \hat{B}_μ decay away from $z=0$. It should also be noted that the frame representation is not unique, yet it minimizes the ℓ_2 norm of the coefficient series $\{\hat{a}_\mu\}$.

Next we consider the special case of the **isodiffracting Gaussian windows**. They are the favorable windows for field processing and propagation for the following reasons; (a) they give rise to the analytically tractable GB propagators in the FD (or to the I-PB in the TD); (b) their width is scaled with the frequency such that they yield the *snuggest frames* for all ω . The simplest isodiffracting window has the form

$$\hat{\psi}_{\text{id}}(\mathbf{x}; \omega) = \exp(-k|\mathbf{x}|^2/2b), \quad \text{where } b > 0. \quad (6)$$

The parameter b is *frequency independent* and is identified as the collimation (Rayleigh) distance of the resulting GB, hence the name isodiffracting. For collimated beams we must choose $kb \gg 1$ for all ω in the band.

Next it is required that the window is to be matched to the frame lattice. Combining the lattice condition (2) with the matching condition (4) using $\Delta_x = (b/k)^{1/2}$ and $\Delta_\xi = (kb)^{-1/2}$, we find that b should be taken such that

$$b = \bar{x}/\bar{\xi} = \bar{k}\bar{x}^2/2\pi = 2\pi/\bar{k}\bar{\xi}^2, \quad \Rightarrow \quad \text{this } b \text{ yields the snuggest frame } \forall \omega < \bar{\omega} \quad (7)$$

As has been shown in [3], for $\nu \lesssim \frac{1}{2}$ the dual window $\hat{\varphi}_{\text{id}}$ corresponding $\hat{\psi}_{\text{id}}$ may be approximated by $(\nu/\|\hat{\psi}\|)^2 \hat{\psi}_{\text{id}}$, giving, via (7), $(\omega/\bar{\omega})^3 (2/\bar{x}^2) \hat{\psi}_{\text{id}}$. For greater ν , $\hat{\varphi}_{\text{id}}$ has a more complicated form and needs to be calculated numerically. Thus, we shall prefer to work in the band $\omega \lesssim \frac{1}{2}\bar{\omega}$ where $\hat{\varphi}_{\text{id}}$ is known analytically and yields localized \hat{a}_μ . This also has an important advantage in the TD algorithm since in this case both $\hat{\psi}$ and $\hat{\varphi}$ have closed form TD counterparts (see (13)). For $\omega \ll \frac{1}{2}\bar{\omega}$, on the other hand, the oversampling is too large and the representation becomes inefficient. Consequently, this formulation is stable and efficient for a frequency band of the order of one octave $\omega \in (\frac{1}{4}\bar{\omega}, \frac{1}{2}\bar{\omega})$ so that the oversampling ratio $(1/\nu)$ is $2 \div 4$. For wider bandwidth we utilize the multiscale formulation in the following section.

2.1 A Multiscale Frame Formulation In The UWB Domain

To overcome the difficulties noted in the previous paragraph for signal bandwidth larger than one octave, we divide the bandwidth into J bands of one octave each (Fig. 2):

$$\Omega^{(j)} = (\bar{\omega}2^{-j-1}, \bar{\omega}2^{-j}), \quad j = 1, \dots, J, \quad \omega_{\text{max}} \leq \bar{\omega}2^{-1}, \quad \omega_{\text{min}} \geq \bar{\omega}2^{-J-1}. \quad (8)$$

For each band, we choose the parameters of the discrete phase space $\mathbf{X}_\mu^{(j)}$ corresponding to the j^{th} band such that

$$\bar{\omega}^{(j)} = \bar{\omega}2^{-j+1}, \quad \text{and} \quad \bar{k}^{(j)}\bar{\xi}^{(j)}\bar{x}^{(j)} = 2\pi, \quad \text{where } \bar{k}^{(j)} = \bar{\omega}^{(j)}/c \quad (9)$$

Subject to this condition we construct $\mathbf{X}_\mu^{(j)}$ for $j > 1$ by decimation of $\mathbf{X}_\mu^{(1)}$ at the highest band, e.g., by choosing

$$(\bar{x}^{(j)}, \bar{\xi}^{(j)}) = (\bar{x}^{(1)}2^{[j/2]}, \bar{\xi}^{(1)}2^{[(j-1)/2]}), \quad \text{where } [\cdot] \text{ denotes the integer part of,} \quad (10)$$

i.e. for every even j the spatial lattice is decimated while the spectral lattice undergoes decimation for odd j . With this choice, the beam lattices for $j > 1$ are obtained by decimations of the lattice at the highest band $j = 1$ (see Fig. 1) hence

the beams need to be traced only once. Finally, from (7), the window parameter for the j^{th} band is $b^{(j)} = \bar{x}^{(j)}/\bar{\xi}^{(j)}$, and subject to (10), $b^{(j)} = b^{(1)}$ or $2b^{(1)}$ for odd or even j , respectively.

3. TIME DOMAIN FRAME FORMULATION: THE BASIC SCHEME

We introduce first the basic TD formulation. Following (2), we define the discretized-space / continuous-time phase space coordinates $\mathbf{Y}_{\mu,\tau} = (\mathbf{x}_m, \boldsymbol{\xi}_n, \tau) = (\mathbf{m}\bar{x}, \mathbf{n}\bar{\xi}, \tau)$ and the corresponding window functions $\psi(\mathbf{x}, t)$ and $\varphi(\mathbf{x}, t)$ to be the TD counterparts (via the inverse Fourier transform) of $\widehat{\psi}(\mathbf{x}, \omega)$ and $\widehat{\varphi}(\mathbf{x}, \omega)$. The TD frames corresponding to (3) are

$$\psi_{\mu,\tau}(\mathbf{x}, t) = \psi[\mathbf{x} - \mathbf{x}_m, t - \tau - c^{-1}\boldsymbol{\xi}_n \cdot (\mathbf{x} - \mathbf{x}_m)], \quad \varphi_{\mu,\tau}(\mathbf{x}, t) = \varphi[\mathbf{x} - \mathbf{x}_m, t - \tau - c^{-1}\boldsymbol{\xi}_n \cdot (\mathbf{x} - \mathbf{x}_m)]. \quad (11)$$

The TD frame expansion of the initial field $u_0(\mathbf{x}, t)$ and of the propagating field $u(\mathbf{r}, t)$ are, from (5)

$$u_0(\mathbf{x}, t) = \sum_{\mu} \int d\tau a_{\mu}(\tau) \psi_{\mu,\tau}(\mathbf{x}, t), \quad u(\mathbf{r}, t) = \sum_{\mu} \int d\tau a_{\mu}(\tau) B_{\mu,\tau}(\mathbf{r}, t), \quad \text{with } a_{\mu}(\tau) = \langle u_0(\mathbf{x}, t), \varphi_{\mu,\tau}(\mathbf{x}, t) \rangle. \quad (12)$$

The expansion coefficient $a_{\mu}(\tau)$ are the TD counterparts of $\widehat{a}_{\mu}(\omega)$ of (5). In (12) they are calculated directly from the TD data. In view of the functional form of (11), they are readily identified as the L-SST of $u_0(\mathbf{x}, t)$ subject to the window $\varphi_{\mu,\tau}$, sampled at the discrete points \mathbf{x}_m with spectral tilts $\boldsymbol{\xi}_n$ (see Fig. 3). The expression (12) for u_0 is the inverse L-SST with the τ -integration being a convolution. As in (5), $B_{\mu,\tau}(\mathbf{r}, t)$ are the propagating PB fields corresponding to the field $\psi_{\mu,\tau}(\mathbf{x}, t)$ in the $z=0$ plane, and the summation involves only the propagating beams with $|\boldsymbol{\xi}_n| < 1$.

Due to the reasons stated in (6)–(7) we shall use the **I-PB windows**. The corresponding TD windows are obtained by TD inversion of the UWB windows $\widehat{\psi}(\mathbf{x}; \omega) = \widehat{f}(\omega)\widehat{\psi}_{\text{ID}}(\mathbf{x}, \omega)$ and $\widehat{\varphi}(\mathbf{x}; \omega) = \widehat{g}(\omega)\widehat{\varphi}_{\text{ID}}(\mathbf{x}, \omega)$ where \widehat{f} and \widehat{g} should be chosen such that $\widehat{f}(\omega)\widehat{g}^*(\omega) = 1$ for $\omega \in \Omega$. Transforming to the time-domain, using the approximate expression for $\widehat{\varphi}(\mathbf{x}; \omega)$ discussed after (7), the *real* spatio-temporal windows are

$$\psi(\mathbf{x}; t) = \text{Re} \{ \overset{\dagger}{f}(t - i|\mathbf{x}|^2/2bc) \}, \quad \varphi(\mathbf{x}; t) \approx (2/\bar{\omega}^3 \bar{x}^2) \text{Im} \{ \overset{\dagger}{g}'''(t - i|\mathbf{x}|^2/2bc) \} \quad (13)$$

where $\overset{\dagger}{f}$ and $\overset{\dagger}{g}$ are the analytic signals corresponding to the frequency spectra \widehat{f} and \widehat{g} . The temporal windowing in (13) is due to the pulse shape of $\overset{\dagger}{f}(t)$ and $\overset{\dagger}{g}(t)$, while the \mathbf{x} -windowing is due to the negative imaginary part of the time-argument in the analytic signals that increases quadratically with $|\mathbf{x}|$ causing a decay of the signal. The functions $\overset{\dagger}{f}(t)$ and $\overset{\dagger}{g}(t)$ should be chosen such that these windows will converge well for numerical processing of the L-SST in (12). The propagators corresponding to (13) are termed I-PB and are related to the ‘‘complex source PB’’ [2]. Expressions for the propagation and scattering of these PBs in homogeneous or in inhomogeneous media are readily available.

3.1 A Multiscale Frame Formulation In The Time Domain

As noted in Sec. 2.1, the UWB formulation is localized and computationally simple for $\omega < \frac{1}{2}\bar{\omega}$, but it becomes increasingly inefficiency (large oversampling) for $\omega < \frac{1}{4}\bar{\omega}$. Consequently, we introduced there a hierarchy of frequency bands such that the beam lattices at the lower bands are decimated versions of the lattice at the highest band. This concept is extended here to the TD, for the same reasons of preserving both localization and efficiency. We apply the TD formulation of (11)–(13) to each one of the frequency bands in (8), using the phase space beam lattices constructed in (9)–(10). The result is a multiscale hierarchy of space-time windows $\{\psi^{(j)}, \varphi^{(j)}\}_1^J$ corresponding to $\Omega^{(j)}$ in (8). Each scale level is then utilized in the discretized local slant-stack transform (DL-SST) of (12) yielding the coefficients $a_{\mu}^{(j)}(\tau)$, and in the field reconstruction formula of (12) using the propagators $B_{\mu,\tau}^{(j)}(\mathbf{r}, t)$. These operations are schematized in Fig. 3, where the left hand side represents the multiscale DL-SST for two scale levels: j and $j+1$. The set of phase space sampling points and directions at the $j+1$ level is obtained by decimation of those of the j^{th} level, and the corresponding space-time windows (light grey) are wider than those at the j^{th} level (dark grey). Fig. 3(right) schematizes the field reconstruction. Here, the beam lattice at the j^{th} level is described by both the full and the dotted-line arrows, but only the full-line arrows are used at the $j+1$ level. The propagators at the j^{th} level (dark grey) are narrower than at the $j+1$ level (light grey).

The scenario in the previous paragraph describes the basic concepts of our multiscale PB summation formulation. Yet it is noted that the sharp division into frequency bands as in (8) is inconvenient in the TD since it introduces end-point effects that lead to slow decaying (sinc-like) space-time windows. This problem can be remedied by further introducing a set of filter-banks $\{\widehat{f}^{(j)}, \widehat{g}^{(j)}\}_1^J$ that generalizes the filters $(\widehat{f}, \widehat{g})$ of (13) such that it allows for overlapping between the adjacent bands as schematized in Fig. 2 while maintaining a uniform representation of the entire excitation band. Due to space limitation, further details will be provided elsewhere.

4. CONCLUSIONS

Two discretized beam summation schemes for ultra-wideband / short-pulse radiation from apertures were introduced. One

was formulated in the UWB-FD (see (5)) and the other, directly in the TD (see (12)). The corresponding *complete set* of propagators are GB or I-PB respectively, emerging from a discrete set of points and orientations in the aperture. The FD scheme utilizes frequency independent beam lattices (unlike the Gabor scheme), and a set of isodiffracting Gaussian windows that guarantees snuggest frame for all ω . The expansion coefficients are WFT of the source function with respect to the dual functions (5). If the source bandwidth is greater than one octave, efficient representation is obtained by using a hierarchy of one-octave bands (8) such that the beam lattices are thinned versions of the lattice at a highest band (see (10)) so that the beams need to be traced only once.

In the TD scheme, the expansion coefficients are calculated via a DL-SST processing of the time-dependent source distribution (see (12) and Fig. 3(left)) structured around a discrete set of space-time sampling points and orientations. Each sampling point yields an I-PB that propagates in the medium. If the source bandwidth is greater than one octave, efficient representation is obtained by using a multiscale filter bank of space-time I-PB windows with approximately one octave bandwidth, where the wider windows correspond to the lower frequencies. Each window is then applied in the DL-SST processing of the data where for the wider window the DL-SST is performed at a properly decimated set of space-time sampling points and orientations (Fig. 3(left)), giving rise to a decimated set of I-PB propagators (Fig. 3(right)).

REFERENCES

- [1]. B. Steinberg, E. Heyman, and L. Felsen, "Phase space beam summation for time dependent radiation from large apertures: Continuous parameterization" *J. Opt. Soc. Amer. A*, vol. 8, pp. 943–958, June 1991.
- [2] E. Heyman and L. Felsen, "Gaussian beam and pulsed beam dynamics: complex source and spectrum formulations within and beyond paraxial asymptotics," *J. Opt. Soc. Amer. A*, vol. 18, pp. 1588–1610, July 2001.
- [3] A. Shlivinski, E. Heyman, A. Boag, D. Lugara and C. Letrou, "Gabor-frame phase space beam summation formulation for wideband radiation from extended apertures," in *Proc. of URSI Triumf International Symposium on Electromagnetic Theory*, (Victoria, Canada), pp. 71–73, May 2001.
- [4] I. Daubechies, *Ten Lectures on Wavelets*, vol. 61 of *CBMS-NSF Regional Conference Series in Applied Mathematics*.

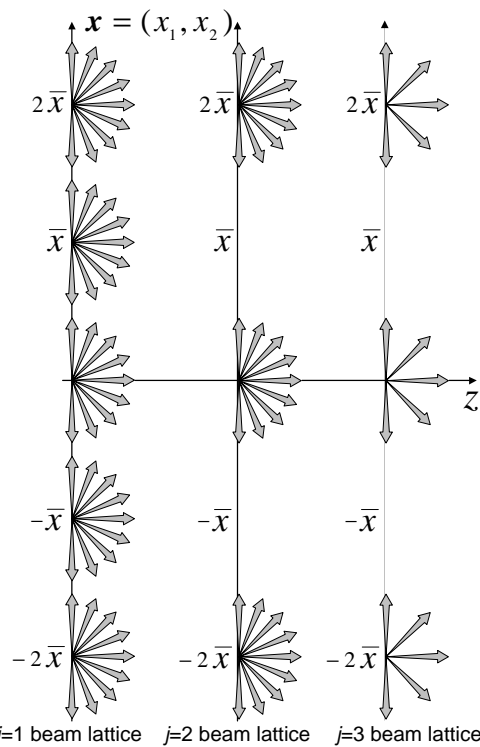


Figure 1. The beam lattices for the $j = 1, 2, 3$ bands.

Following (10), the $j = 2$ lattice is obtained by a spatial decimation of the $j = 1$ lattice, while the $j = 3$ lattice is a spectral decimation of the $j = 2$ lattice.

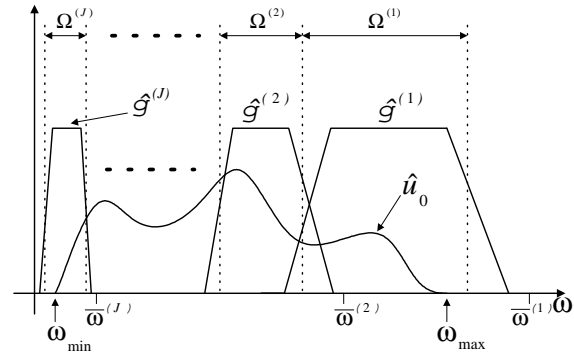


Figure 2. Frequency domain construction of the filter bank $\{\hat{g}^{(j)}\}_1^J$. Each $\Omega^{(j)}$ has a one-octave bandwidth.

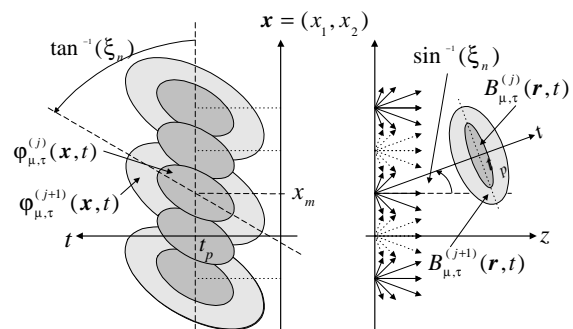


Figure 3. Left hand side: The j and the $j + 1$ levels multiscale DL-SST. The phase space lattice (locations/orientations/times) at the $j + 1$ level is obtained by decimation of the j^{th} level lattice and the space-time windows of the former ($\varphi_{\mu,\tau}^{(j+1)}$; light grey) are wider than those of the latter (dark grey). **Right hand side:** Field reconstruction. All the arrows are used at the j^{th} level, but only the full-line arrows are used at the $j + 1$ level (see Fig. 1). The propagators $B_{\mu,\tau}^{(j+1)}$ of the $j + 1$ level (light grey) are wider than those of the j level (dark grey).